Tracking the Time Evolution of the Electron Distribution Function in Copper by Femtosecond Broadband Optical Spectroscopy

Manuel Obergfell and Jure Demsar
Institute of Physics, Johannes Gutenberg-University Mainz, 51099 Mainz, Germany

(Received 25 February 2019; revised manuscript received 17 November 2019; published 21 January 2020)

Multitemperature models are nowadays often used to quantify the ultrafast electron-phonon (boson) relaxations and coupling strengths in advanced quantum solids. To test their applicability and limitations, we perform systematic studies of carrier relaxation dynamics in copper, a prototype system for which the two-temperature model (TTM) was initially considered. Using broadband time-resolved optical spectroscopy, we study the time evolution of the electron distribution function, $f(E)$, over a large range of excitation densities. Following intraband optical excitation, $f(E)$ is found to be athermal over several 100 fs, with a substantial part of the absorbed energy already being transferred to the lattice. We show, however, that the electron-phonon coupling constant can still be obtained using the TTM analysis, provided that the data are analyzed over the time window where the electrons are already quasithermal, and the electronic temperature is determined experimentally.

DOI: 10.1103/PhysRevLett.124.037401

Cooperative phenomena in quantum solids arise from a delicate balance among interactions between charge, spin, and lattice degrees of freedom. The knowledge of the interaction strengths between the different subsystems is thus crucial for their understanding. The knowledge of the Eliashberg electron-boson coupling constant λ is of particular interest in novel superconductors, as it provides information on the significance of the electron-boson interaction (or the lack thereof) for superconducting pairing. One of the approaches to determine λ is to use femtosecond (fs) time-resolved techniques [1]. Here, fs optical pulses are used to excite the electronic system, while the recovery dynamics is probed by measuring the resulting transient changes in optical constants [2] or the electronic occupation near the Fermi energy [3,4]. Considering simple metals and assuming the electron-electron (e-e) thermalization being much faster than the electron-phonon (e-ph) relaxation, the so-called two-temperature model (TTM) has been put forward [1,5]. Within this description, the electrons rapidly thermalize to a temperature T_e, which is much higher than that of the lattice, T_l. This process is followed by the e-ph thermalization on a timescale $\tau_{e\text{-}ph}$, inversely proportional to the e-ph coupling strength [1,5]. This widely used model suggests a simple relationship between the measured $\tau_{e\text{-}ph}$ and λ, when experiments are performed above the Debye temperature $T_l \gtrsim \Theta_D$. With the electronic specific heat $C_e = \gamma T_e$, where γ is the Sommerfeld constant, the time evolutions of T_e and T_l are given by a set of coupled heat equations [1,6,7]. Here [1]

$$\frac{1}{\tau_{e\text{-}ph}} = \frac{3\hbar\lambda\langle\omega^2\rangle}{\pi k_B T_e}\left(1 - \frac{\hbar^2\langle\omega^4\rangle}{12\langle\omega^2\rangle k_B^2 T_e T_l} + \cdots\right), \quad (1)$$

where $\lambda\langle\omega^n\rangle = 2\int_0^\infty [\alpha^2F(\Omega)/\Omega]\Omega^n d\Omega$, while $\alpha^2F(\Omega)$ is the product of the e-ph coupling strength α^2 and the phonon density of states F. Often the Debye approximation is used, where α^2 is mode independent. In this case, $\lambda\langle\omega^2\rangle$ is simply the product of λ and the mean square phonon frequency, $\langle\omega^2\rangle$.

Following pioneering works on noble metals [13–18], numerous time-resolved experiments on superconductors have been performed, ranging from conventional [2] to high-T_c cuprate [3,19–23] and pnictide [24,25] superconductors, aiming at the determination of λ. Similar studies were performed also on other advanced materials ranging from carbon nanotubes [4] and ferromagnets [26] to metallic nanoparticles [27]. Despite the reasonable agreement between the experimentally extracted and theoretically estimated values of $\lambda\langle\omega^2\rangle$ [2], numerous studies shed doubts on the applicability of the TTM. The time-resolved photoemission data on Au showed that even at room temperature and high excitation densities, the e-e thermalization time is as long as 800 fs, while the electronic distribution at earlier times is strongly athermal [28]. The TTM prediction that in the limit of weak excitations $\tau_{e\text{-}ph} \propto T_l^{-3}$ as $T_l \to 0$ K was never observed in simple metals [29,30]. The absence of slowing down of relaxation at low-T_l and long e-e thermalization times were both attributed to Pauli blocking, where e-e scattering into states below the Fermi level (E_F) is reduced due to the small fraction of unoccupied states to which electrons can be scattered [29,30]. Unlike in Dirac systems like graphene, where electrons are indeed found to thermalize on the sub-50-fs timescale [31–33], several recent studies suggest the e-e and e-ph thermalization timescales to actually be

comparable [34–36]. To account for the nonthermal electron distributions, several extensions of the TTM have been put forward [18,29,37–42].

In this Letter, we present an all-optical approach to study the time evolution of the photoinduced changes in the electronic distribution function near the Fermi energy, $\Delta f(E-E_F)$, in thin copper films. We achieve this by studying the temporal evolution of the complex dielectric function, $\varepsilon(\omega)=\varepsilon_1(\omega)+i\varepsilon_2(\omega)$, following intraband photoexcitation. In Cu, $\varepsilon(\omega)$ is in the visible spectral range largely governed by the interband transition from the d band to the Fermi level. With the combination of static $\varepsilon(\omega)$, thermomodulation, $\Delta\varepsilon(\omega)=[d\varepsilon(\omega)/dT]\Delta T$, and the simple model of the electronic density of states, which accounts for $\varepsilon(\omega,T)$, we demonstrate that $\Delta f(E,t)$ can be extracted from $\Delta\varepsilon(\omega,t)$. We show that in Cu the $f(E)$ is quasithermal only for time delays beyond $\approx$0.5 ps. Moreover, the experimentally determined T_e's are—for short time delays—substantially lower than the expected values based on the absorbed energy density. This implies a substantial energy transfer to the lattice already in the early stage of relaxation. Despite the obvious disparity of the presented results and the TTM, we demonstrate that the TTM analysis can yield a consistent value of $\lambda\langle\omega^2\rangle$, providing that (i) the data are analyzed at time delays when the electron subsystem is already quasithermal, and (ii) the T_e's are recorded experimentally. The presented approach could be generalized to other systems with interband optical transitions in the visible range.

The broadband femtosecond time-resolved optical studies were performed on thin (24 nm) Cu films sputtered on (100) MgO substrate. The reflectivities (Re) and transmissions (Tr) of films were measured with commercial FTIR and UV-Vis spectrometers. The measured optical constants were found to be in good agreement with literature values [43]. The samples were photoexcited by 50-fs near-infrared (NIR) pulses ($\lambda_{pe}=800$ nm, 1.55 eV). The absorbed energy densities, U, calculated from the measured $\varepsilon(1.55\text{ eV})$ [7], were varied between 4 and 250 J/cm^3. The photoinduced changes of both Tr and Re between 1.25 and 2.8 eV were measured with white-light supercontinuum pulses generated in sapphire [44]. Combining the static $\varepsilon(\omega)$ and the measured transient changes in reflectivity and transmission, ΔRe/Re and ΔTr/Tr, respectively, $\Delta\varepsilon(\omega,t)$ is determined by numerically solving a system of appropriate Fresnel equations [7,45,46].

Figure 1 shows the time evolution of ΔTr/Tr and ΔRe/Re of a 24-nm-thick Cu film on MgO substrate, recorded at room temperature, in the spectral range between 1.25 and 2.8 eV. The equilibrium Re and Tr are presented in the inset to Fig. 1(a). The anomaly centered at $\approx$2.1 eV is a result of the interband transition ($\mathcal{T}_{d\text{-}p}$) between the d band, located at $\mathcal{E}_{d\text{-}p}=2.1$ eV below the Fermi level, and the Cu s-p band. The time-resolved data show strong changes in optical properties near $\mathcal{E}_{d\text{-}p}$, arising from photoinduced

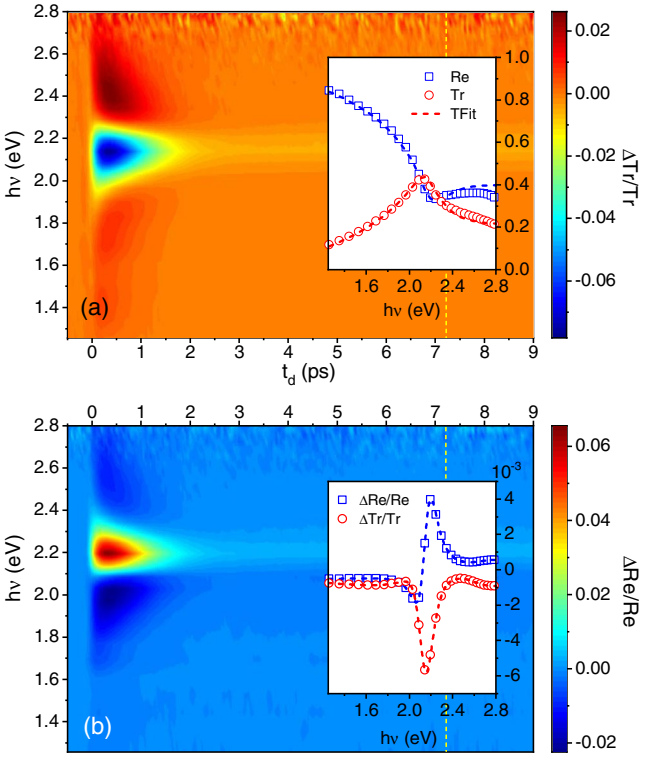

FIG. 1. Dynamics of (a) the ΔTr/Tr and (b) the ΔRe/Re of a 24-nm-thick Cu film on MgO substrate excited by a 50-fs NIR pulse. The base temperature is 300 K, and the excitation fluence is $F=3.4$ mJ/cm^2, corresponding to the absorbed energy density $U=54$ J/cm^3. The inset to panel (a) presents Re and Tr (open symbols), together with the corresponding model fits (dashed lines). The inset to panel (b) presents ΔRe/Re and ΔTr/Tr at 7.2 ps (open symbols) together with the thermomodulation fits (dashed lines).

changes in $\mathcal{T}_{d\text{-}p}$ [47]. Since the NIR pump pulse excites the s-p-band electrons, it is the photoinduced Fermi-level smearing—i.e., the broadening of the electronic distribution near E_F—that is mainly responsible for changes in $\mathcal{T}_{d-p}$ [see Fig. 2(a)]. Assuming the validity of the TTM, T_e should reach $\approx$1100 K at $U=54$ J/cm^3 [7]. Following the e-e and e-ph thermalization processes, a quasiequilibrium is reached within a few picoseconds (the photoinduced spectra show no measurable changes between 5 and 30 ps). The subsequent decay is governed by the heat diffusion into the substrate. Therefore, we can assume that $\Delta\varepsilon(\omega,t\gtrsim 5\text{ ps})=[d\varepsilon(\omega)/dT]\Delta T$, where ΔT is the resulting temperature increase, given by $U=\int_{T_0}^{T_0+\Delta T}C_p(T)dT$, where $C_p(T)$ is the total specific heat. Indeed, the recorded ΔTr/Tr(7 ps) and ΔRe/Re(7 ps), shown in the inset to Fig. 1(b), match well the changes obtained by simply heating up the sample using a hot plate (conventional thermomodulation). For $U=54$ J/cm^3, we obtain $\Delta T\approx 15$ K.

As noted, the dominant contribution to changes in the optical constants in the visible range stems from the photoinduced Fermi level smearing. It results in opening/blocking

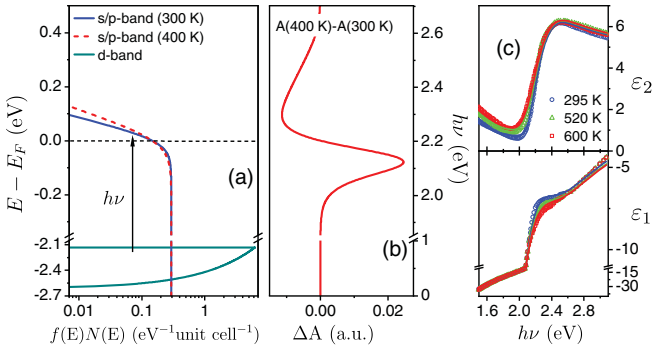

FIG. 2. The thermomodulation of optical constants in Cu, modeled by a simplified model of the density of states and the Fermi golden rule. Panel (a) presents the modeled occupied density of states in Cu (note the semilogarithmic scale) at 300 and 400 K. The corresponding changes in absorption are presented in (b). They are dominated by the changes in the interband transition between the fully occupied d band and the s-p conduction band. The model is applied in (c) to fit (solid lines) the published spectroscopic ellipsometry data on Cu [48] taken at different temperatures (open symbols).

the optical transitions from the fully occupied d band at $\approx$2.1 eV below E_F, to s-p band states below/above the E_F [47], as sketched in Fig. 2(a). Thus, a proper parametrization of $\varepsilon(\omega, T)$ provides means to access changes in the electronic distribution function—and also for time delays where the distribution is athermal.

To model the equilibrium and the thermomodulation optical spectra in the visible range [7], we consider $\varepsilon(\omega, T) = \varepsilon_D(\omega, T) + \varepsilon_{d\text{-}p}(\omega, T) + \varepsilon_\infty(T)$. Here $\varepsilon_D(\omega)$ is the free carrier Drude response of the s/p electrons, and $\varepsilon_{d\text{-}p}(\omega)$ describes the interband transition between the uppermost d band and the s-p band, while ε_∞ sums up the contributions of higher-energy interband transitions to $\varepsilon(\omega, T)$. All contributions are T dependent. The T dependence of $\varepsilon_D(\omega)$ is governed by the T dependence of the Drude scattering rate, γ_D [7], which is governed by the e-ph scattering above 300 K, where γ_D depends linearly on T_l. The changes due to the Fermi level smearing are, for the thermomodulation, sketched in Fig. 2(b). They give rise to a bipolar change in the interband absorption near $\mathcal{E}_{d\text{-}p}$, with the amplitude proportional to ΔT_e. In addition, a small shift of $\mathcal{E}_{d\text{-}p}$ can be expected, either due to the shift of the chemical potential (proportional to ΔT_e) or due to the thermal lattice expansion (proportional to ΔT_l). In Cu, the electronic DOS at E_F is nearly constant and the former can be neglected; thus the shift in $\mathcal{E}_{d\text{-}p}$ is governed by T_l. Finally, the induced changes in higher-energy interband transitions (> 4 eV) may also contribute to $\Delta\varepsilon(\omega)$ in the visible range. These changes, driven by the thermal expansion ($\propto \Delta T_l$), give rise to a weak frequency-independent offset in the real part of $\Delta\varepsilon(\omega)$ [7]. The findings are tested on published optical data [48] in Fig. 2(c).

Since only $\Delta\varepsilon_{d\text{-}p}(\omega, T)$ is dominated by $\Delta f(E, t)$, and ΔT_l is much smaller than ΔT_e, we can parametrize the changes of $\varepsilon(\omega)$ that are a result of ΔT_l, thereby getting access to $\Delta f(E, t)$. We start by modeling the equilibrium $\varepsilon(\omega, T)$, to account for Tr and Re at room temperature, as well as for the bolometric responses. The latter is given by $\Delta\mathrm{Tr}/\mathrm{Tr}(t \gtrsim 5\ \mathrm{ps})$ and $\Delta\mathrm{Re}/\mathrm{Re}(t \gtrsim 5\ \mathrm{ps})$ and was recorded at 12 different excitation levels with $4 < U < 250\ \mathrm{J/cm^3}$. To model $\varepsilon_{d\text{-}p}(\omega, T)$, which dominates $\Delta\varepsilon(\omega)$ in the visible range, we developed a simple model (see Ref. [7]) considering the Fermi golden rule, and using the band dispersions that give rise to densities of states of the d band and the s-p band, as shown in Fig. 2(a). For the Drude scattering rate, γ_D, and $\mathcal{E}_{d\text{-}p}$, we assume they depend linearly on lattice temperature [e.g., $\gamma_D(300K + \Delta T_l) = \gamma_{D,300K} + c_\gamma \Delta T_l$]. Such a linear expansion is justified, since the maximal changes in the lattice temperature (for highest U) are of the order of $\Delta T_l = 60$ K. We determined these parameters by globally fitting $\varepsilon(\omega)$ and $\Delta\varepsilon(\omega, t \gtrsim 5\ \mathrm{ps})$ for U, spanning nearly 2 orders of magnitude. The resulting $\varepsilon(\omega, T)$ is shown to describe well Tr and Re [inset to Fig. 1(a)], as well as the thermomodulation response [inset to Fig. 1(b)].

To determine $\Delta f(E, t)$ from experimental data, we assume that $\Delta T_l = \Delta T_l(t \gtrsim 5\ \mathrm{ps})[1 - \exp(-t/\tau)]$, where τ is the decay time of the spectrally averaged transient. Both experimental studies [49] and detailed numerical calculations [50] demonstrated that the phonon subsystem is also athermal on the picosecond timescale. However, the relatively small contribution of the components linked to changes in T_l to the overall changes in $\varepsilon(\omega)$ makes the result relatively insensitive to the variation of τ. With this, and the extracted coefficients describing $\gamma_D(T_l)$, $\varepsilon_\infty(T_l)$, $\mathcal{E}_{d\text{-}p}(T_l)$, we obtain $\Delta f(E, t)$ by fitting the model to the experimental data.

Figures 3(a) and 3(b) present the time evolution of Δf extracted from the data shown in Fig. 1. To evaluate $\Delta f(E, t)$, we first compare the experimental Δf around E_F with the best fit assuming thermalized electrons, where $\Delta f_{FD} = f(E, T_e) - f(E, 300\ \mathrm{K})$, and T_e is obtained by the best fit of Δf_{FD} to the experimental Δf. The normalized error $\delta(t) = \sum |\Delta f(E, t) - \Delta f_{FD}(E, t)| / \sum |\Delta f_{FD}(E, t)|$, where the sum spans the data for $-0.4\ \mathrm{eV} \lesssim E - E_F \lesssim 0.4$ eV, is shown in the inset to Fig. 3(c) for two excitation densities. $\delta(t)$ decreases by about 1 order of magnitude within the time delay that we attribute to the e-e thermalization time, $\tau_{e\text{-}e}$. From that point on, the value is roughly constant [note that $\Delta f(E, t) - \Delta f_{FD}(E, t)$ at individual energies are added by their absolute values]. Figure 3(c) addresses the excitation dependence of $\tau_{e\text{-}e}$ obtained from the analysis of $\delta(t)$. In particular, we plot the times $t_\delta(U)$, where $\delta(t)$ reach different levels between the maximum $\delta_{\max} = 1$ and its minimum, $\delta_{\min} \approx 0.1$. All of the curves show the same trend, all suggesting that $\tau_{e\text{-}e}$ time is reduced by a factor of $\approx$3 between $U \sim 30\ \mathrm{J/cm^3}$ and

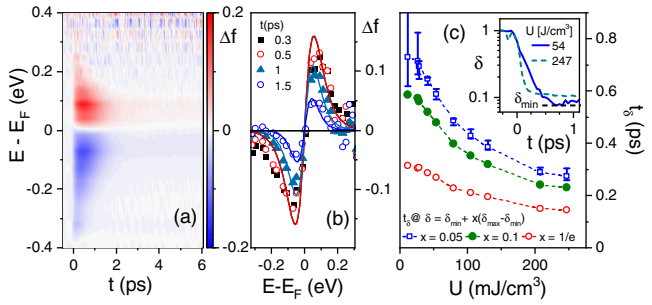

FIG. 3. Analysis of the time-resolved optical data at $U = 54$ J/cm^3. Panel (a) shows $\Delta f(E,t)$ following the photoexcitation, while (b) shows Δf at selected time delays. Panel (c) presents the U dependence of the e-e thermalization obtained through the analysis of $\delta(t)$ (see inset). Different values correspond to different reductions of $\delta(t)$. For clarity, we show the error bars for $x = 0.05$ only.

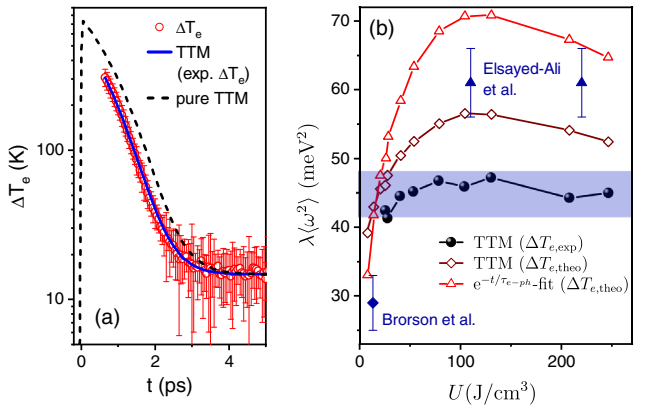

FIG. 4. (a) The time evolution of extracted ΔT_e (open red circles), where ΔT_e is obtained by fitting the Δf data [Figs. 3(a) and 3(b)] with Δf_{FD}. The data are fit using the TTM (solid blue line). For comparison, we present the prediction of the pure TTM (dashed line), with the initial T_e calculated from U. (b) The $\lambda\langle\omega^2\rangle$ extracted from $\Delta T_e(t)$ obtained at different U's. It is independent on U, as expected. For comparison, we present $\lambda\langle\omega^2\rangle(U)$, obtained by assuming the validity of the TTM (i.e., by using ΔT_e^{theo}), fit by either the full TTM or by a single exponential decay (see text). The corresponding published values [2,17] are included for comparison.

$U \sim 300$ J/cm^3. The long $\tau_{e\text{-}e}$ at low excitation densities [$\tau_{e\text{-}e} \approx 700$ fs, considering $\tau_{e\text{-}e}$ as the time when $\delta(t)$ reaches $\delta_{\min} + 0.05(\delta_{\max} - \delta_{\min})$] seems to be the main reason for the departure of the observed relaxation dynamics from the standard TTM. The observed trend is consistent with the relaxed Pauli blocking for high excitation densities, and in line with calculations using Boltzmann collision integrals [51]. It follows that for $U \sim 50$ J/cm^3, the $f(E,t)$ reaches the quasithermal state only on the timescale of ≈600 fs, while for $U \sim 250$ J/cm^3 the timescale is reduced to ≈250 fs.

Figure 4(a) presents the time evolution of the extracted electronic temperature ($U = 54$ J/cm^3) from the point where $f(E,t)$ is quasithermal. Analyzing experimental $\Delta T_e(t > 0.6$ ps) using the TTM (solid blue line), where $\Delta T_l(t = 0.6$ ps) was determined by the energy conservation law [7], we obtain $\lambda\langle\omega^2\rangle = 45$ meV^2, in excellent agreement with theoretical estimates [52]. The dashed line in Fig. 4(a) presents the pure TTM simulation with the same value of $\lambda\langle\omega^2\rangle$ and $\Delta T_{e,\text{theo}}(t = 0)$ determined from the absorbed energy density via $\Delta T_{e,\text{theo}}(t{=}0) = \sqrt{T_l^2 + 2U/\gamma} - T_l$. The measured ΔT_e's are, throughout the thermalization process, substantially lower than those expected from the pure TTM. This implies a substantial energy transfer to the phonon subsystem already before the electrons thermalize. The rapid relaxation of energy to the phonon bath during the early stage of relaxation can be attributed to the fact that for high-energy electrons, the energy-momentum conservation restrictions for the e-ph relaxation are lifted compared to the case of low-energy (thermal) electrons. I.e., for e-ph scattering of high-energy electrons, there are plenty of available final states to relax to, which is not the case for the relaxation of electrons close to the Fermi level. We note that in the early relaxation stage, the density of photoexcited carriers remains constant while energy is transferred to the lattice.

Not being able to properly determine ΔT_e can be a major source of error in estimating $\lambda\langle\omega^2\rangle$. Thus, the values of $\lambda\langle\omega^2\rangle$ obtained by time-resolved methods vary substantially, depending on the underlying assumptions used in the data analysis. For time delays when electrons are quasithermal, we used the TTM analysis on the extracted $\Delta T_e(t)$. $\lambda\langle\omega^2\rangle$ values for data taken at different U's are shown in Fig. 4(b) with black spheres. As expected for moderate excitations [51,53], $\lambda\langle\omega^2\rangle$ is found to be U independent. However, applying the common approach of extracting $\lambda\langle\omega^2\rangle$ with $T_{e,\text{theo}}(t = 0)$ and fitting the recovery by either (i) an exponential decay and Eq. (1), or (ii) the full TTM fit, the extracted $\lambda\langle\omega^2\rangle$ is shown to strongly vary with U. The previously published values [2,17] follow this trend.

Our study demonstrates that, for simple metals with weak e-ph coupling, $\lambda\langle\omega^2\rangle$ can be extracted using the TTM, provided that the analysis is restricted to times where the electronic distribution is quasithermal, and that T_e's are measured. Such studies should be performed as a function of U to demonstrate the consistency with the TTM predictions.

In numerous advanced solids, the carrier relaxation is found to proceed on a sub-picosecond timescale, with U-independent dynamics [21]. It was argued that, in the low-U limit, the e-e thermalization may actually be slower than the e-ph relaxation over most of the accessible temperatures [39,40]. An alternative expression, linking the measured $\tau_{e\text{-}ph}$ and $\lambda\langle\omega^2\rangle$ for such nonthermal cases has been derived [39,40]. The derived expression, $\lambda\langle\omega^2\rangle = 2\pi k_B T_l/3\hbar\tau_{e\text{-}ph}$, is nearly identical to Eq. (1), with T_e

replaced by $2T_l$. Applying this model to the low-U data on Cu, where the extracted $\tau_{e\text{-}e}$ is comparable to $\tau_{e\text{-}ph}$ [7], we obtain $\lambda\langle\omega^2\rangle = 50$ meV^2. The good agreement between the two approaches may suggest that the density at which the recovery dynamics start to be U dependent corresponds to the point where $\tau_{e\text{-}e} \lessapprox \tau_{e\text{-}ph}$.

Even for simple metals, the literature values of $\lambda\langle\omega^2\rangle$, extracted from the time-resolved data, vary by as much as a factor of 2—depending on the excitation density and the approximation used. While this factor may appear to be small, we note that this difference may correspond to the change between the strong and weak e-ph coupling [54]. The all-optical approach, where time evolution of the electronic distribution function in a thin film can be recorded, may provide a way to extracting λ's also in advanced solids.

This work was supported by the Carl-Zeiss Stiftung and the DFG in the framework of the Collaborative Research Centre SFB TRR 173, "Spin +X." We gratefully acknowledge valuable discussions with V. V. Kabanov and B. Rethfeld.

[1] P. B. Allen, Phys. Rev. Lett. **59**, 1460 (1987).
[2] S. D. Brorson, A. Kazeroonian, J. S. Moodera, D. W. Face, T. K. Cheng, E. P. Ippen, M. S. Dresselhaus, and G. Dresselhaus, Phys. Rev. Lett. **64**, 2172 (1990).
[3] L. Perfetti, P. A. Loukakos, M. Lisowski, U. Bovensiepen, H. Eisaki, and M. Wolf, Phys. Rev. Lett. **99**, 197001 (2007).
[4] T. Hertel, R. Fasel, and G. Moos, Appl. Phys. A **75**, 449 (2002).
[5] M. I. Kaganov, I. M. Lifshitz, and L. V. Tantarov, Zh. Exsp. Theor. Fiz. **31**, 232 (1956) [Sov. Phys. JETP **4**, 173 (1957)].
[6] J. Demsar and T. Dekorsy, in *Optical Techniques for Solid-State Materials Characterization*, edited by R. P. Prasankumar and A. J. Taylor (Francis & Taylor, New York, 2011).
[7] See the Supplemental Material at http://link.aps.org/supplemental/10.1103/PhysRevLett.124.037401 for detailed description of modelling of the optical response of Cu, the determination of excitation density and the comparison to the data analysis using pure TTM, which includes Refs. [8–12].
[8] M. Dressel and G. Grüner, *Electrodynamics of Solids: Optical Properties of Electrons in Matter* (Cambridge University Press, New York, 2002).
[9] J. F. Janak, A. R. Williams, and V. L. Moruzzi, Phys. Rev. B **11**, 1522 (1975).
[10] R. D. Averitt and A. J. Taylor, J. Phys. Condens. Matter **14**, R1357 (2002).
[11] N. E. Phillips, CRC Crit. Rev. Solid State Sci. **2**, 467 (1971).
[12] D. L. Martin, Rev. Sci. Instrum. **58**, 639 (1987).
[13] G. L. Eesley, Phys. Rev. Lett. **51**, 2140 (1983).
[14] J. G. Fujimoto, J. M. Liu, E. P. Ippen, and N. Bloembergen, Phys. Rev. Lett. **53**, 1837 (1984).
[15] R. W. Schoenlein, W. Z. Lin, J. G. Fujimoto, and G. L. Eesley, Phys. Rev. Lett. **58**, 1680 (1987).
[16] H. E. Elsayed-Ali, T. B. Norris, M. A. Pessot, and G. A. Mourou, Phys. Rev. Lett. **58**, 1212 (1987).
[17] H. E. Elsayed-Ali and T. Juhasz, Phys. Rev. B **47**, 13599 (1993).
[18] C. K. Sun, F. Vallee, L. H. Acioli, E. P. Ippen, and J. G. Fujimoto, Phys. Rev. B **50**, 15337 (1994).
[19] S. D. Brorson, A. Kazeroonian, D. W. Face, T. K. Cheng, G. L. Doll, M. S. Dresselhaus, G.Dresselhaus, E. P. Ippen, T. Venkatesan, X. D. Wu, and A. Inam, Solid State Commun. **74**, 1305 (1990).
[20] S. V. Chekalin, V. M. Farztdinov, V. V. Golovlyov, V. S. Letokhov, Yu. E. Lozovik, Yu. A. Matveets, and A. G. Stepanov, Phys. Rev. Lett. **67**, 3860 (1991).
[21] C. Gadermaier, A. S. Alexandrov, V. V. Kabanov, P. Kusar, T. Mertelj, X. Yao, C. Manzoni, D. Brida, G. Cerullo, and D. Mihailovic, Phys. Rev. Lett. **105**, 257001 (2010).
[22] S. Dal Conte, C. Giannetti, G. Coslovich, F. Cilento, D. Bossini, T. Abebaw, F. Banfi, G. Ferrini, H. Eisaki, M. Greven, A. Damascelli, D. van der Marel, and F. Parmigiani, Science **335**, 1600 (2012).
[23] E. E. M. Chia, D. Springer, S. K. Nair, X. Q. Zou, S. A. Cheong, C. Panagopoulos, T. Tamegai, H. Eisaki, S. Ishida, S. Uchida, A. J. Taylor, and J.-X. Zhu, New J. Phys. **15**, 103027 (2013).
[24] B. Mansart, D. Boschetto, A. Savoia, F. Rullier-Albenque, F. Bouquet, E. Papalazarou, A. Forget, D. Colson, A. Rousse, and M. Marsi, Phys. Rev. B **82**, 024513 (2010).
[25] L. Stojchevska, P. Kusar, T. Mertelj, V. V. Kabanov, X. Lin, G. H. Cao, Z. A. Xu, and D. Mihailovic, Phys. Rev. B **82**, 012505 (2010).
[26] E. Carpene, E. Mancini, C. Dallera, M. Brenna, E. Puppin, and S. De Silvestri, Phys. Rev. B **78**, 174422 (2008).
[27] C. Voisin, D. Christofilos, P. A. Loukakos, N. Del Fatti, F. Vallée, J. Lermé, M. Gaudry, E. Cottancin, M. Pellarin, and M. Broyer, Phys. Rev. B **69**, 195416 (2004).
[28] W. S. Fann, R. Storz, H. W. K. Tom, and J. Bokor, Phys. Rev. Lett. **68**, 2834 (1992); Phys. Rev. B **46**, 13592 (1992).
[29] R. H. M. Groeneveld, R. Sprik, and A. Lagendijk, Phys. Rev. B **51**, 11433 (1995).
[30] K. H. Ahn, M. J. Graf, S. A. Trugman, J. Demsar, R. D. Averitt, J. L. Sarrao, and A. J. Taylor, Phys. Rev. B **69**, 045114 (2004).
[31] D. Brida, A. Tomadin, C. Manzoni, Y. J. Kim, A. Lombardo, S. Milana, R. R. Nair, K. S. Novoselov, A. C. Ferrari, G. Cerullo, and M. Polini, Nat. Commun. **4**, 1987 (2013).
[32] I. Gierz, F. Calegari, S. Aeschlimann, M. Chávez Cervantes, C. Cacho, R. T. Chapman, E. Springate, S. Link, U. Starke, C. R. Ast, and A. Cavalleri, Phys. Rev. Lett. **115**, 086803 (2015).
[33] G. Rohde, A. Stange, A. Müller, M. Behrendt, L.-P. Oloff, K. Hanff, T. J. Albert, P. Hein, K. Rossnagel, and M. Bauer, Phys. Rev. Lett. **121**, 256401 (2018).
[34] P. Kusar, V. V. Kabanov, S. Sugai, J. Demsar, T. Mertelj, and D. Mihailovic, Phys. Rev. Lett. **101**, 227001 (2008).
[35] A. Pashkin, M. Porer, M. Beyer, K. W. Kim, A. Dubroka, C. Bernhard, X. Yao, Y. Dagan, R. Hackl, A. Erb, J. Demsar, R. Huber, and A. Leitenstorfer, Phys. Rev. Lett. **105**, 067001 (2010).
[36] M. Beyer, D. Städter, M. Beck, H. Schäfer, V. V. Kabanov, G. Logvenov, I. Bozovic, G. Koren, and J. Demsar, Phys. Rev. B **83**, 214515 (2011).

[37] M. Lisowski, P. A. Loukakos, U. Bovensiepen, J. Stähler, C. Gahl, and M. Wolf, Appl. Phys. A **78**, 165 (2004).
[38] E. Carpene, Phys. Rev. B **74**, 024301 (2006).
[39] V. V. Kabanov and A. S. Alexandrov, Phys. Rev. B **78**, 174514 (2008).
[40] V. V. Baranov and V. V. Kabanov, Phys. Rev. B **89**, 125102 (2014).
[41] G. Della Valle, M. Conforti, S. Longhi, G. Cerullo, and D. Brida, Phys. Rev. B **86**, 155139 (2012).
[42] E. A. A. Pogna, S. Dal Conte, G. Soavi, V. G. Kravets, Y.-J. Kim, S. Longhi, A. N. Grigorenko, G. Cerullo, and G. Della Valle, ACS Photonics **3**, 1508 (2016).
[43] P. B. Johnson and R. W. Christy, Phys. Rev. B **6**, 4370 (1972).
[44] R. R. Alfano, *The Supercontinuum Laser Source: Fundamentals With Updated References*, 2nd ed. (Springer, 2006).
[45] M. A. Dupertuis, B. Acklin, and M. Proctor, J. Opt. Soc. Am. A **11**, 1159 (1994).
[46] M. A. Dupertuis, B. Acklin, and M. Proctor, J. Opt. Soc. Am. A **11**, 1167 (1994).
[47] R. Rosei and D. W. Lynch, Phys. Rev. B **5**, 3883 (1972).
[48] L. J. Hanekamp, W. Lisowski, and G. A. Bootsma, Surf. Sci. **118**, 1 (1982).
[49] L. Waldecker, R. Bertoni, R. Ernstorfer, and J. Vorberger, Phys. Rev. X **6**, 021003 (2016).
[50] P. Maldonado, K. Carva, M. Flammer, and P. M. Oppeneer, Phys. Rev. B **96**, 174439 (2017).
[51] B. Y. Mueller and B. Rethfeld, Phys. Rev. B **87**, 035139 (2013).
[52] T. P. Beaulac, P. B. Allen, and F. J. Pinski, Phys. Rev. B **26**, 1549 (1982).
[53] Z. Lin, L. V. Zhigilei, and V. Celli, Phys. Rev. B **77**, 075133 (2008).
[54] P. B. Allen and B. Mitrovic, Solid State Phys. **37**, 1 (1983).